

Naphthalimide-containing coordination polymer with mechanoresponsive luminescence and excellent metal ion sensing properties

Jian-Jun Liu,*^a Shu-Biao Xia,^a Qi-Tao Que,^a Hongbo Suo,^b Jiaming Liu,^c Xiang Shen^a and Fei-Xiang Cheng *^a

^a*Center for Yunnan-Guizhou Plateau Chemical Functional Materials and Pollution Control,
Qujing Normal University, Qujing 655011, China.*

^b*School of Pharmacy, Liaocheng University, Liaocheng, Shandong 252059, China.*

^c*School of Metallurgy Engineering, Jiangxi University of Science and Technology, Ganzhou
341000, PR China*

E-mail: jjliu302@163.com (J.-J. Liu); chengfx2010@163.com (F.-X. Cheng)

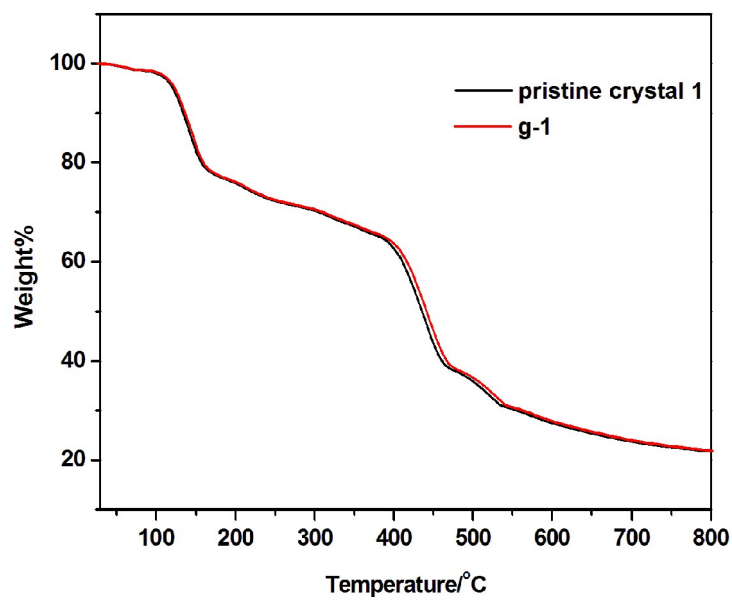


Fig. S1. TGA curves of pristine crystal 1 and its ground sample g-1.

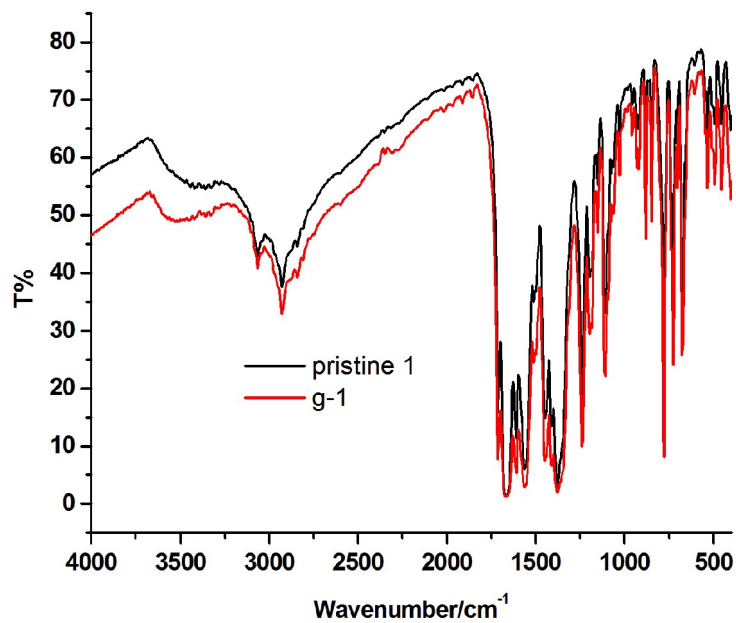


Fig. S2. FT-IR (ATR) spectra of pristine 1 and g-1.

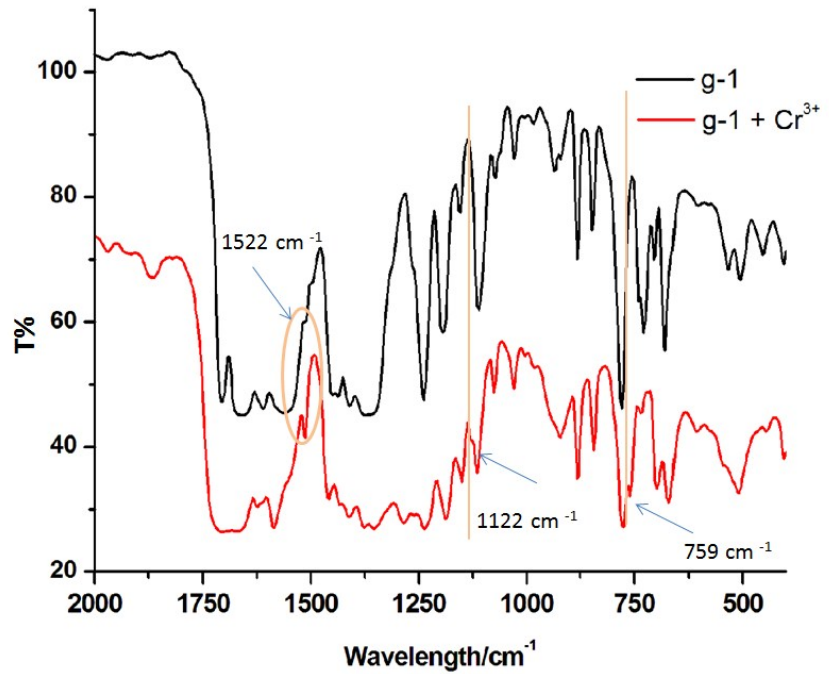


Fig. S3. FT-IR spectra of g-1 and g-1+Cr³⁺

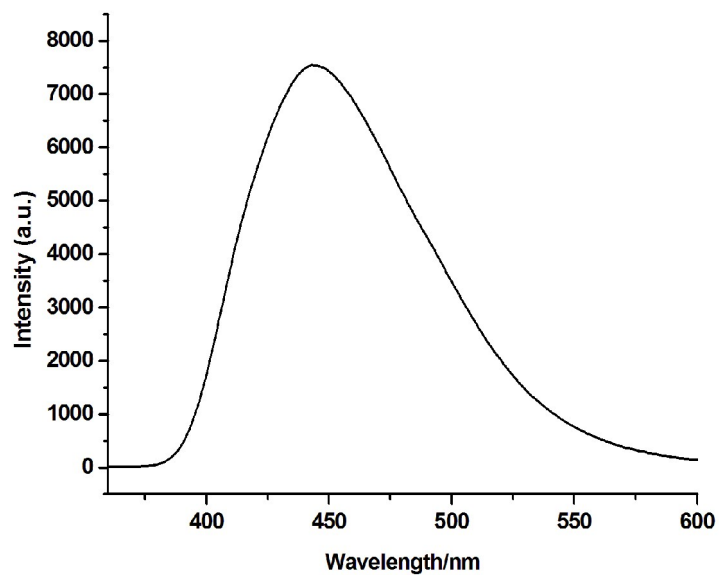


Fig. S4. Emission spectra of solid state H₂INI ($\lambda_{\text{ex}} = 320 \text{ nm}$).

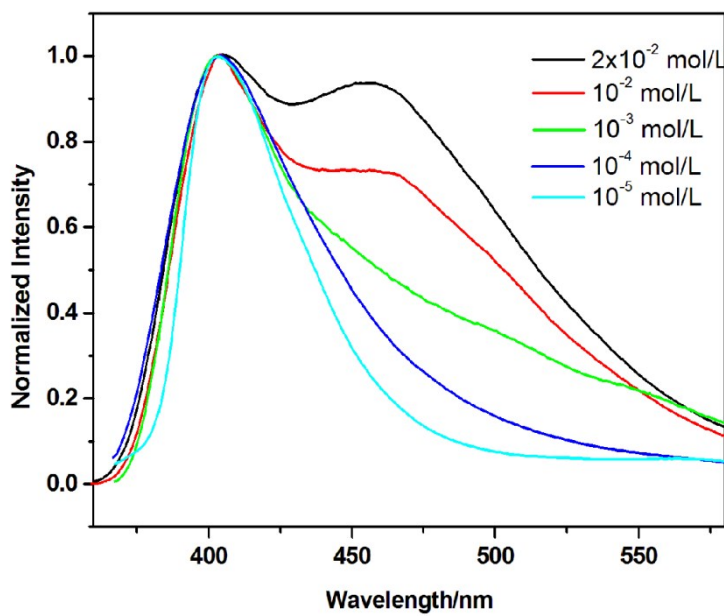


Fig. S5. Emission spectra of the H_2INI in DMF solution ($\lambda_{\text{ex}} = 320$ nm).

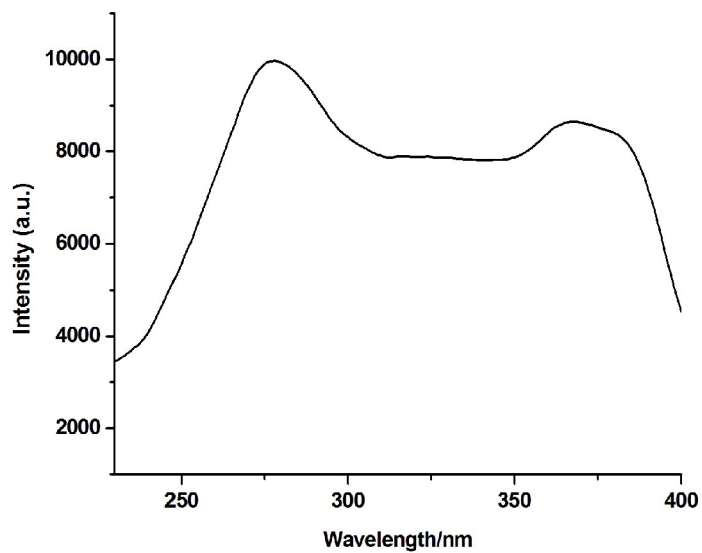


Fig. S6. Excitation spectra of the H_2INI ($\lambda_{\text{em}} = 443$ nm).

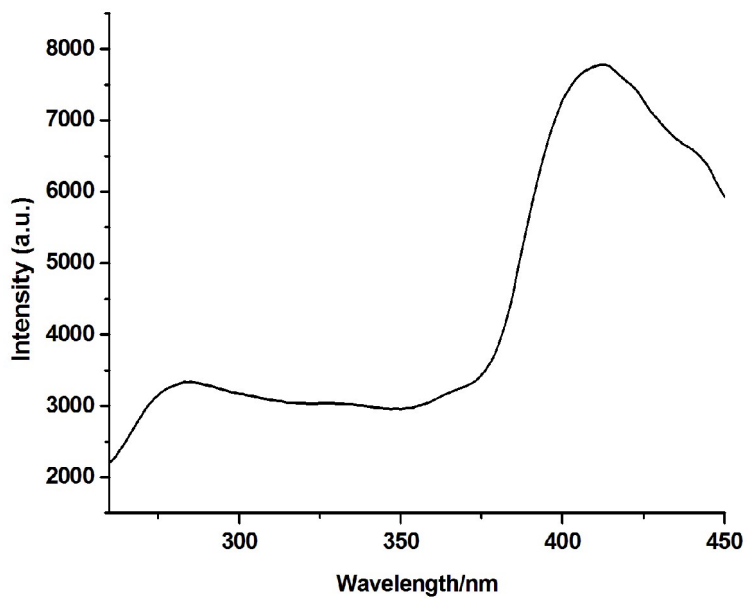


Fig. S7. Excitation spectra of the pristine crystal **1** ($\lambda_{\text{em}} = 501$ nm).

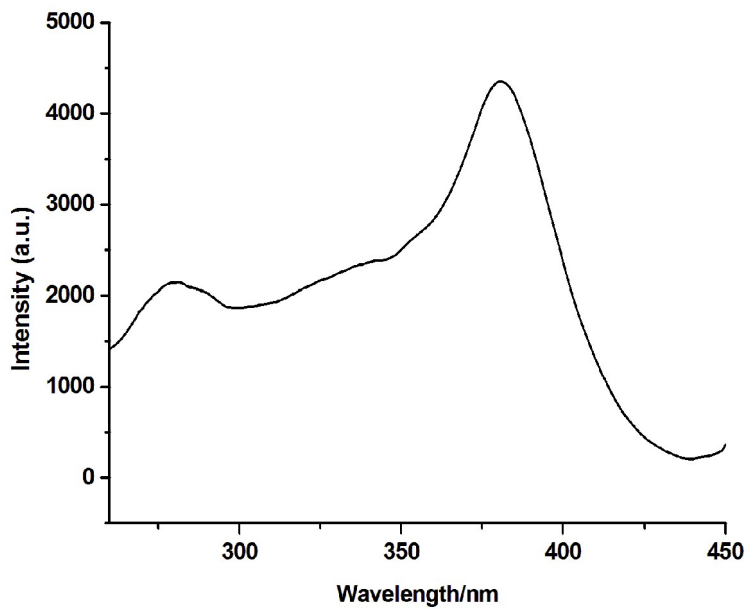


Fig. S8. Excitation spectra of the **g-1** ($\lambda_{\text{em}} = 458$ nm).

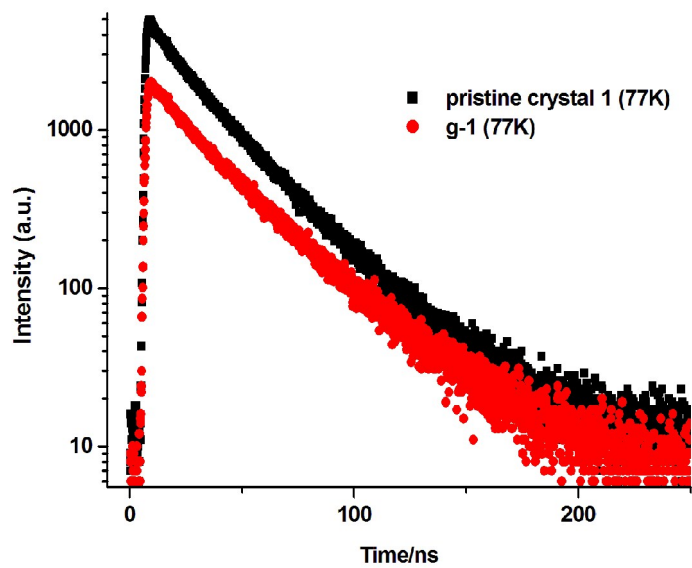


Fig. S9. Fluorescence decay curves of the pristine crystal **1** and **g-1** at 77 K.

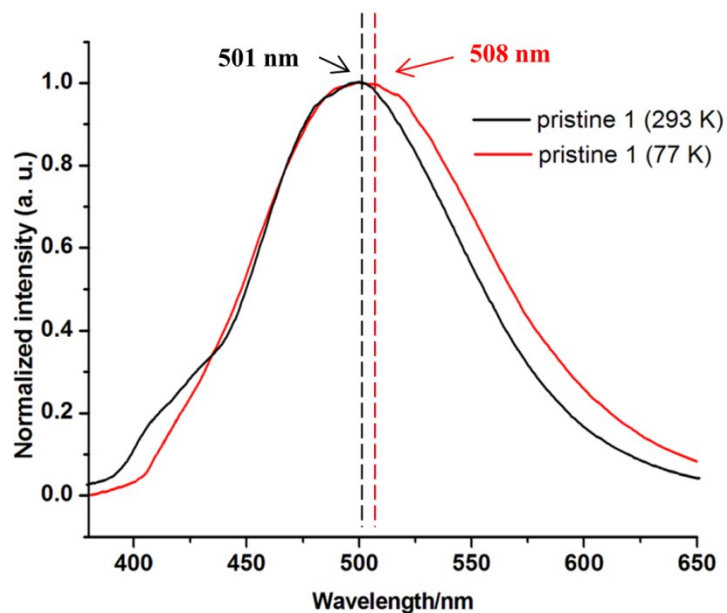


Fig. S10. Emission spectra of pristine crystal **1** at 293 K and 77 K ($\lambda_{\text{ex}} = 320 \text{ nm}$)

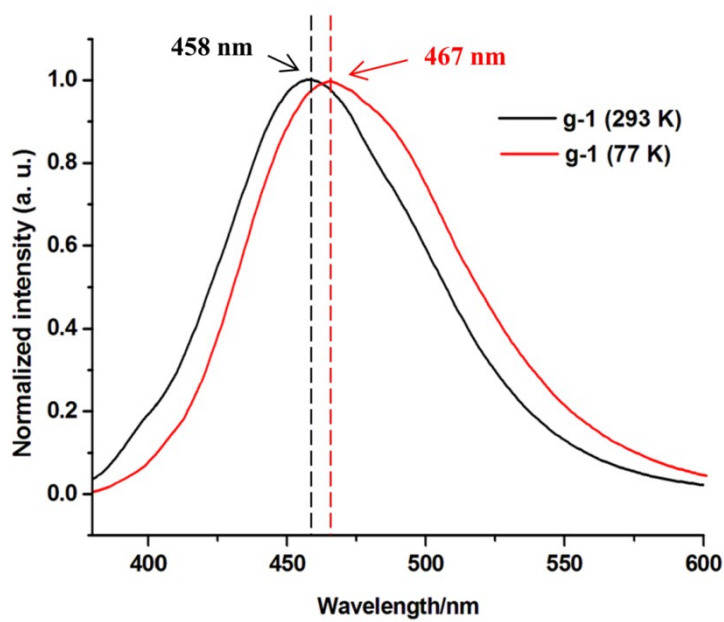


Fig. S11. Emission spectra of the g-1 at 293 K and 77 K ($\lambda_{\text{ex}} = 320 \text{ nm}$)

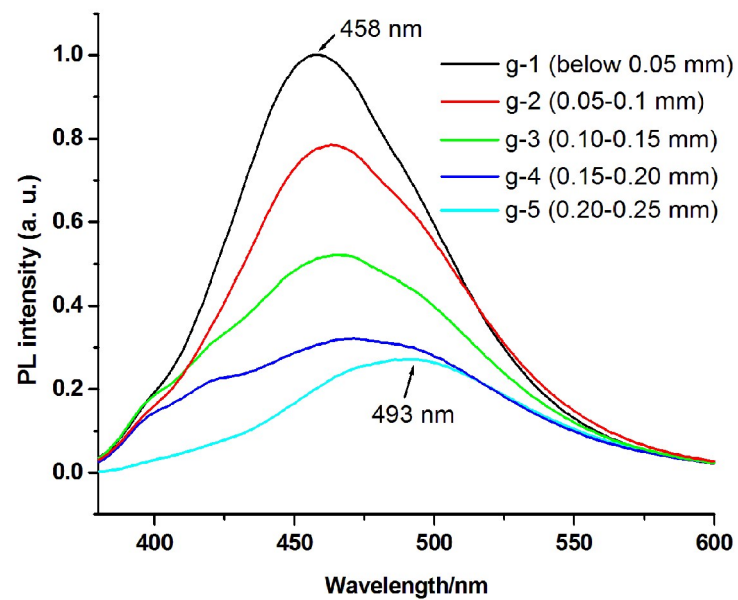


Fig. S12. Emission spectra of different-sized ground samples ($\lambda_{\text{ex}} = 320 \text{ nm}$).

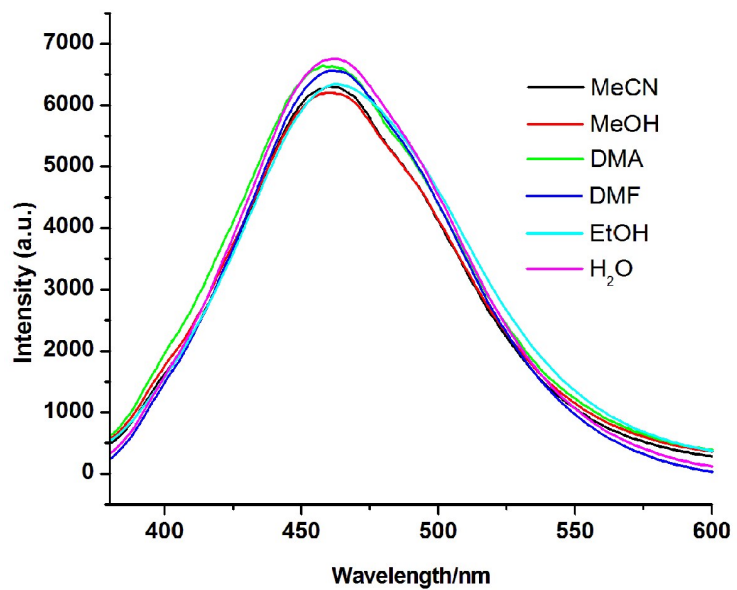


Fig. S13. Emission spectra of g-1 dispersed in various pure solvents ($\lambda_{\text{ex}} = 320 \text{ nm}$).

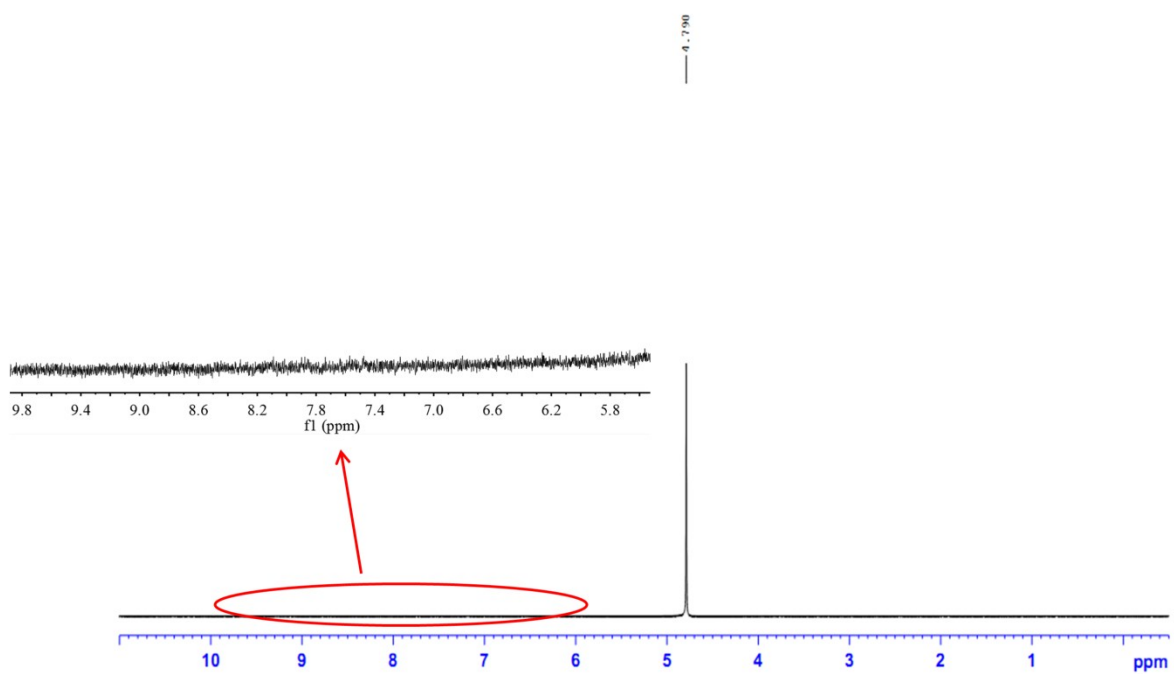


Fig. S14 ¹H NMR spectra of the deuterated water extract of g-1.

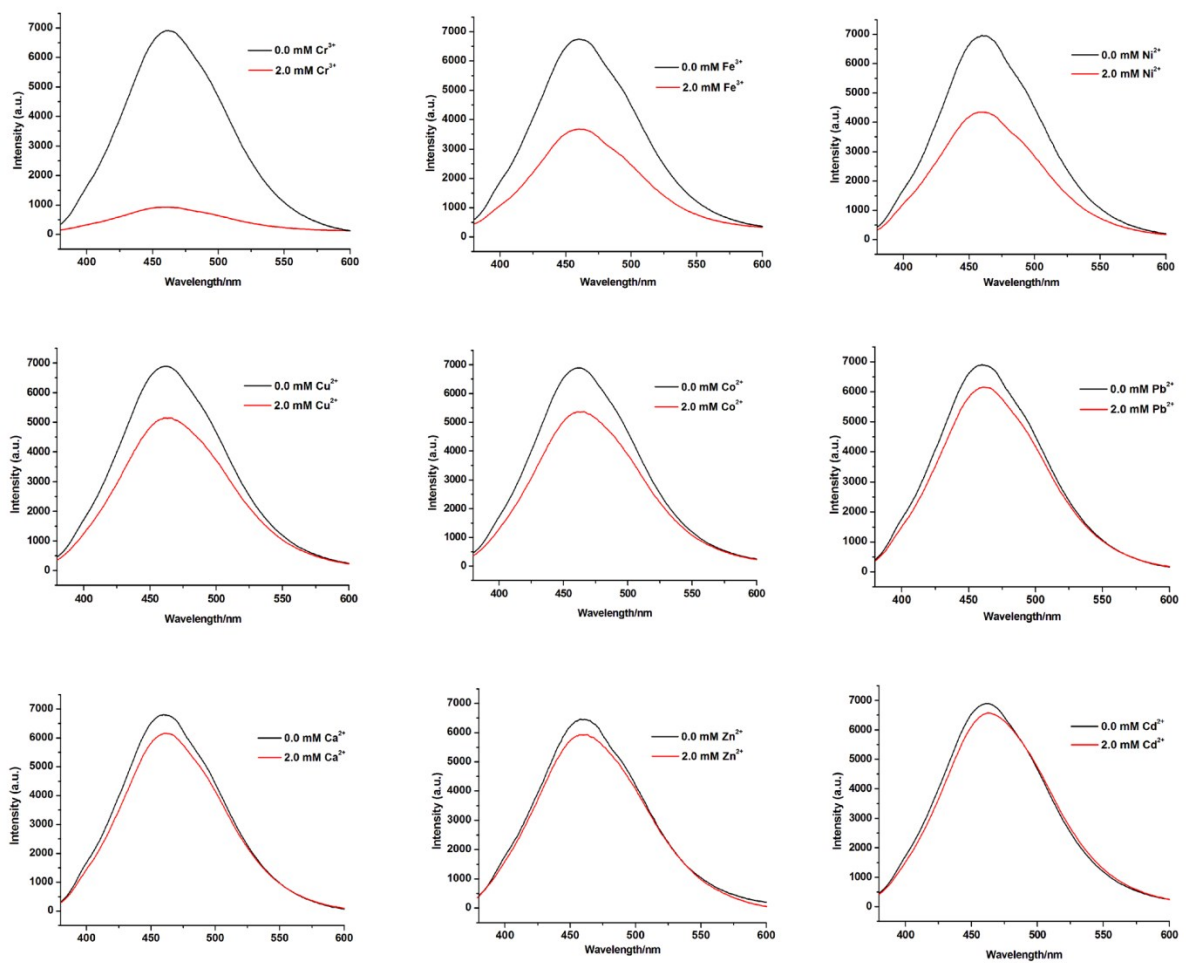


Fig. S15. Families of various Emission spectra of g-1 in aqueous solution upon the addition of 2.0 mM of different selected metal ions ($\lambda_{\text{ex}} = 320 \text{ nm}$).

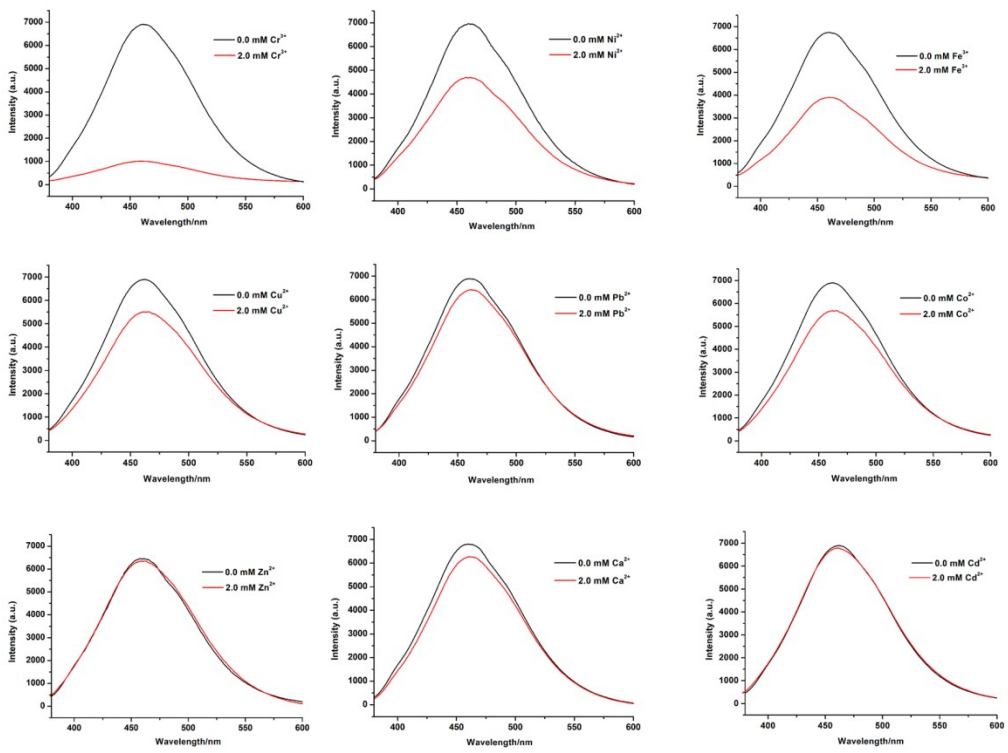


Fig. S16. Families of various Emission spectra of g-1 in aqueous solution upon the addition of 2.0 mM of different selected metal ions ($\lambda_{\text{ex}} = 340 \text{ nm}$).

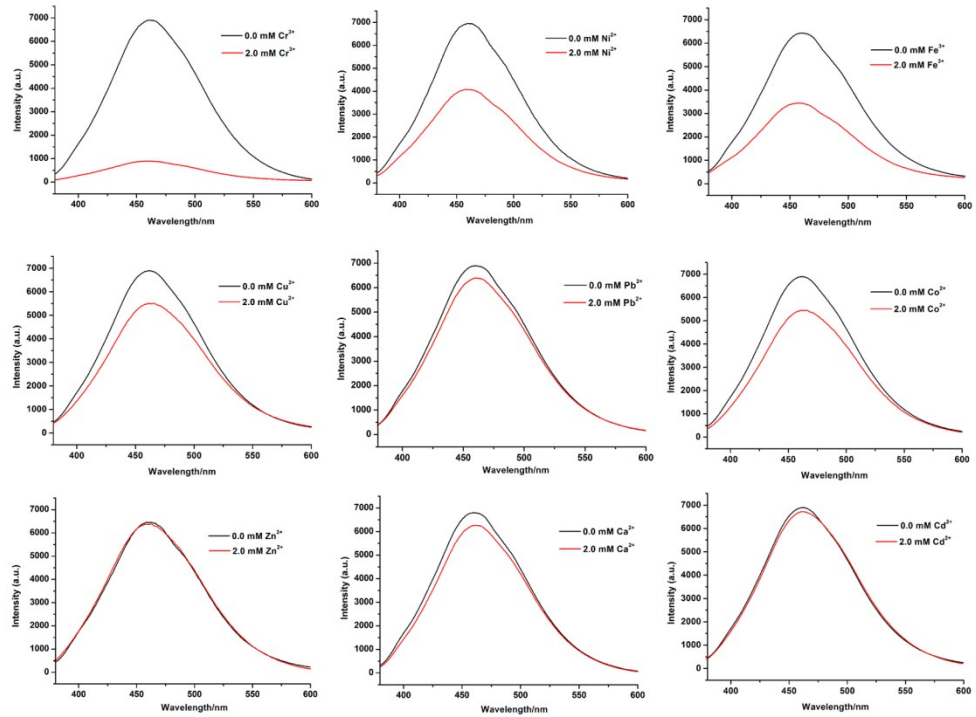


Fig. S17. Families of various Emission spectra of g-1 in aqueous solution upon the addition of 2.0 mM of different selected metal ions ($\lambda_{\text{ex}} = 360 \text{ nm}$).

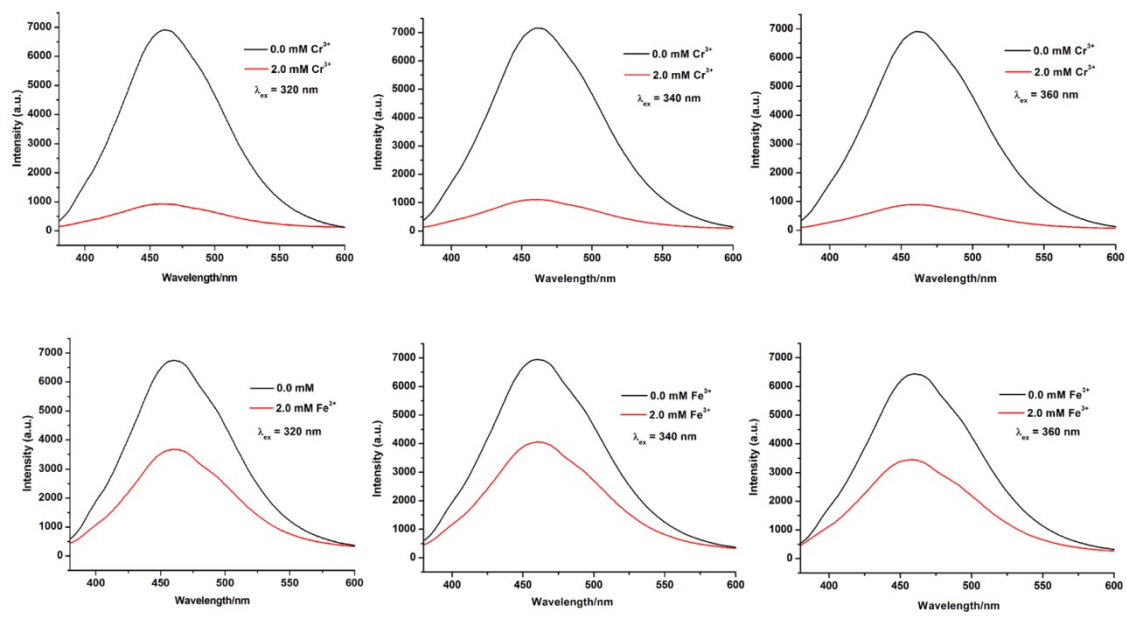


Fig. S18. Emission spectra of **g-1** in Fe³⁺ and Cr³⁺ aqueous solution under different excitation wavelengths.

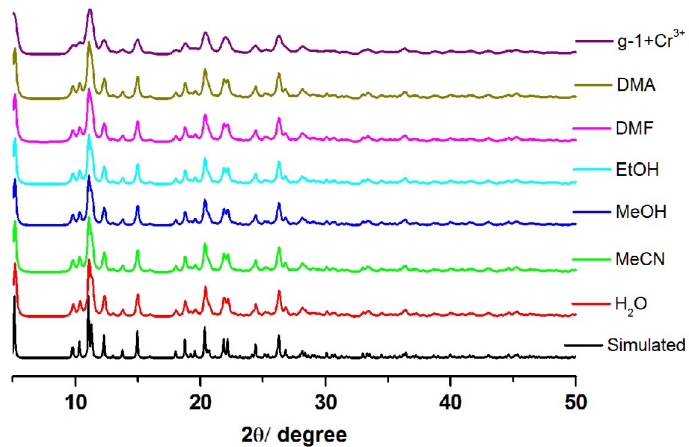


Fig. S19. PXRD patterns of **g-1** after soaking in Cr³⁺ ion and various common solvents.

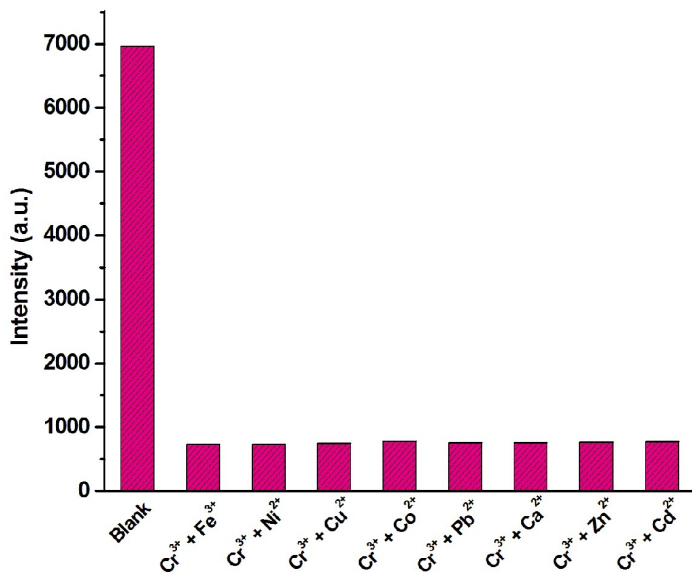


Fig. S20. Comparison of the luminescence intensity of Cr^{3+} in the presence of mixed metal ions for g-1.

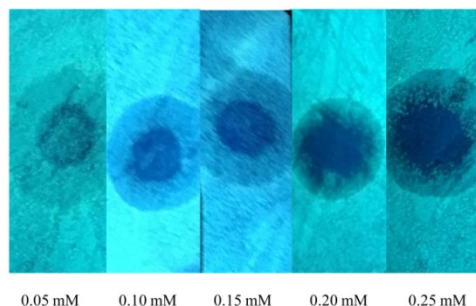


Fig. S21. Photographs of the g-1 test paper after treated with different concentrations of Cr^{3+} ions (under a 365 nm UV lamp).

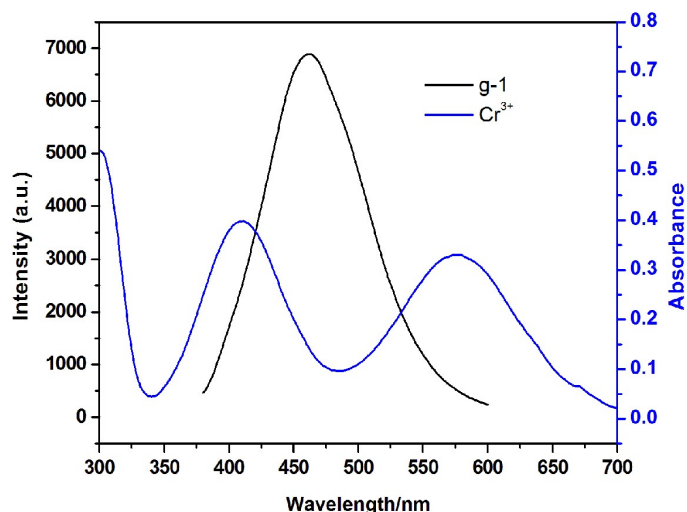


Fig. S22. The UV-vis absorption spectrum of Cr^{3+} and the emission spectrum of g-1.

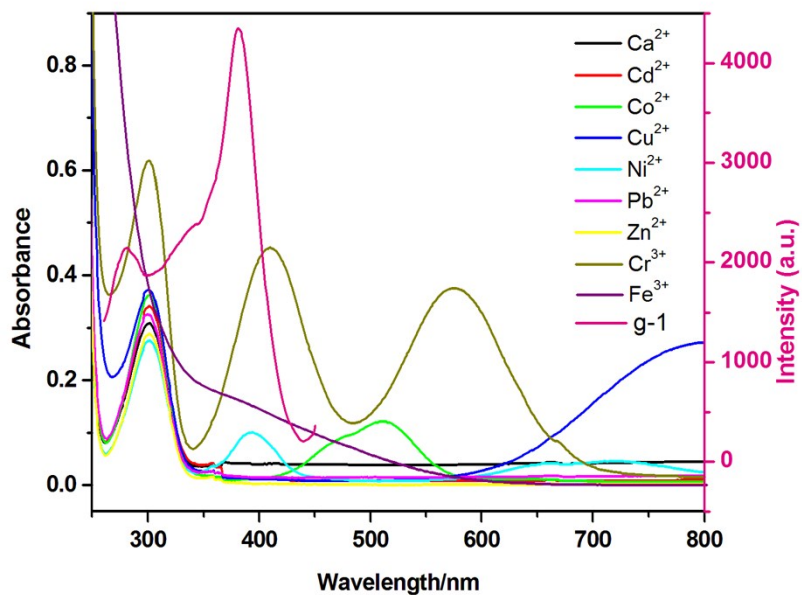


Fig. S23. The UV-vis absorption spectra of metal ions and the excitation spectrum of g-1.

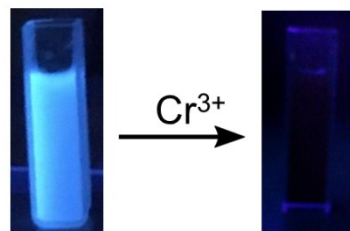


Fig. S24. Photographs show the luminescence change of g-1 in presence of Cr³⁺ (3.5 mM).

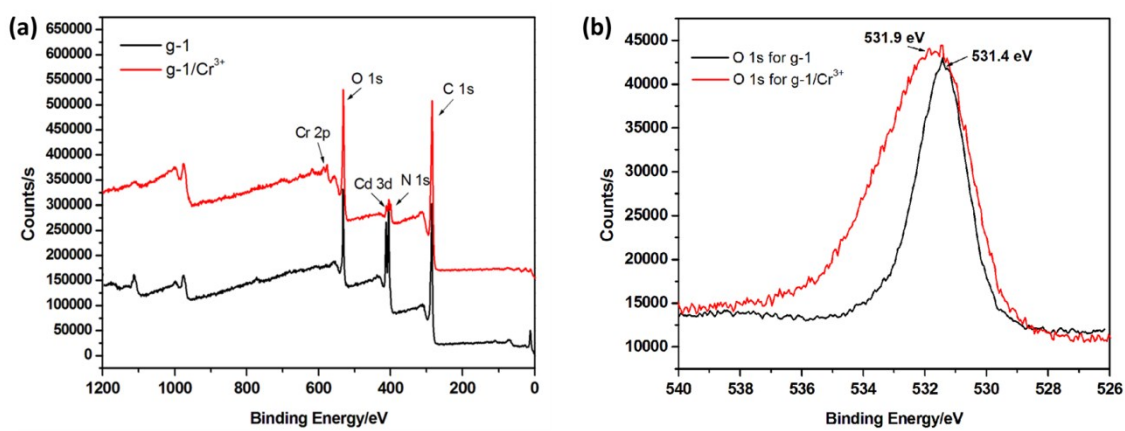


Fig. S25. (a) XPS for g-1 and g-1/Cr³⁺; (b) O 1s XPS for g-1 and g-1/Cr³⁺.

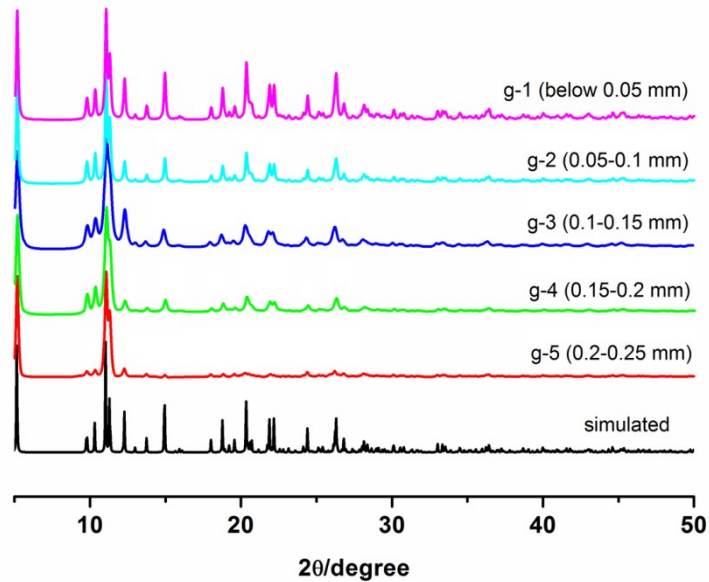


Fig. S26. PXRD patterns for the several ground samples with different grinding degree.

Table S1. Bond lengths [\AA] and angles [°] for complex 1.

Cd1—O1	2.2638 (12)	Cd1—O3 ⁱⁱ	2.3383 (12)
Cd1—O2 ⁱ	2.2708 (12)	Cd1—O4 ⁱⁱ	2.3832 (12)
Cd1—O8	2.3068 (13)	Cd1—C8 ⁱⁱ	2.6894 (17)
Cd1—O7	2.3253 (14)		
O1—Cd1—O2 ⁱ	127.12 (4)	O2 ⁱ —Cd1—O4 ⁱⁱ	85.35 (4)
O1—Cd1—O8	89.60 (5)	O8—Cd1—O4 ⁱⁱ	106.12 (5)
O2 ⁱ —Cd1—O8	93.49 (5)	O7—Cd1—O4 ⁱⁱ	81.86 (5)
O1—Cd1—O7	84.42 (5)	O3 ⁱⁱ —Cd1—O4 ⁱⁱ	55.79 (4)
O2 ⁱ —Cd1—O7	85.84 (5)	O1—Cd1—C8 ⁱⁱ	118.50 (5)
O8—Cd1—O7	171.92 (5)	O2 ⁱ —Cd1—C8 ⁱⁱ	112.91 (5)
O1—Cd1—O3 ⁱⁱ	92.50 (5)	O8—Cd1—C8 ⁱⁱ	99.67 (5)
O2 ⁱ —Cd1—O3 ⁱⁱ	140.21 (4)	O7—Cd1—C8 ⁱⁱ	87.97 (5)
O8—Cd1—O3 ⁱⁱ	89.95 (5)	O3 ⁱⁱ —Cd1—C8 ⁱⁱ	27.99 (5)
O7—Cd1—O3 ⁱⁱ	95.72 (5)	O4 ⁱⁱ —Cd1—C8 ⁱⁱ	27.82 (5)
O1—Cd1—O4 ⁱⁱ	143.56 (5)		

Symmetry codes: (i) $-x+1, -y+2, -z+1$; (ii) $-x+1, -y+1, -z+1$.